

## Probing carbon impurities in hexagonal boron nitride epilayers

M. R. Uddin, J. Li, J. Y. Lin, and H. X. Jiang<sup>a)</sup>

Department of Electrical and Computer Engineering, Texas Tech University, Lubbock, Texas 79409, USA

(Received 9 February 2017; accepted 15 April 2017; published online 2 May 2017)

Carbon doped hexagonal boron nitride epilayers have been grown by metal organic chemical vapor deposition. Photocurrent excitation spectroscopy has been utilized to probe the energy levels associated with carbon impurities in hexagonal boron nitride (*h*-BN). The observed transition peaks in photocurrent excitation spectra correspond well to the energy positions of the bandgap, substitutional donors ( $C_B$ , carbon impurities occupying boron sites), and substitutional acceptors ( $C_N$ , carbon impurities occupying nitrogen sites). From the observed transition peak positions, the derived energy level of  $C_B$  donors in *h*-BN is  $E_D \sim 0.45$  eV, which agrees well with the value deduced from the temperature dependent electrical resistivity. The present study further confirms that the room temperature bandgap of *h*-BN is about 6.42–6.45 eV, and the  $C_N$  deep acceptors have an energy level of about 2.2–2.3 eV. The results also infer that carbon doping introduces both shallow donors ( $C_B$ ) and deep acceptors ( $C_N$ ) via self-compensation, and the energy level of carbon donors appears to be too deep to enable carbon as a viable candidate as an n-type dopant in *h*-BN epilayers. Published by AIP Publishing. [<http://dx.doi.org/10.1063/1.4982647>]

As a member of the III-nitride wide bandgap semiconductor family, boron nitride (BN) is a much less matured material in comparison to GaN and AlN. Hexagonal boron nitride (*h*-BN) is highly promising as a deep-ultraviolet (DUV) photonic material exhibiting extremely high optical absorption and emission,<sup>1–8</sup> as an ideal material for the exploration of two-dimensional heterojunction devices,<sup>9–11</sup> and as a solid-state neutron detector material.<sup>12,13</sup> Previous theoretical and experimental studies have revealed that the energy bandgap and the free exciton binding energy of this material are very large and are around 6.4–6.5 eV and 0.7–0.75 eV, respectively.<sup>1–8,14–21</sup> Recent realization of wafer-scale semiconducting *h*-BN epilayers with high crystalline and optical qualities has opened up opportunities for the exploration of fundamental properties and emerging applications of this ultra-wide bandgap semiconductor. For instance, by employing photocurrent spectroscopy studies, the room temperature bandgap ( $E_g$ ), binding energy of excitons ( $E_{bx}$ ), and binding energy of acceptor-bound-excitons ( $E_{bx}$ ) in *h*-BN epilayers have been directly determined from the observed transition peak positions to be  $E_g \sim 6.42$  eV,  $E_x \sim 0.73$  eV, and  $E_{bx} \sim 0.2$  eV, respectively.<sup>22</sup> Neutron detectors fabricated from B-10 enriched *h*-BN epilayers have demonstrated the highest thermal neutron detection efficiency to date among solid-state neutron detectors of 51.4%.<sup>12</sup>

More comprehensive studies on the impurity properties for *h*-BN produced under controlled growth conditions are still needed to provide input for approaches towards material quality improvement, to eliminate undesired defects, and to understand issues concerning possible doping approaches. Nitrogen vacancies ( $V_N$ ) and carbon impurities occupying nitrogen sites ( $C_N$ ) are known to be two of the most common defects in *h*-BN.<sup>23–31</sup> Based on the photoluminescence (PL) emission spectroscopy studies performed on unintentionally doped *h*-BN epilayers grown under varying  $NH_3$  flow rates

(hence with controlled  $V_N$  concentrations)<sup>32,33</sup> and theoretical insights,<sup>24–28</sup> it is now understood that  $V_N$  are shallow donors with an activation energy of about 0.1 eV, whereas  $C_N$  are deep acceptors having two activation energies of about 2.3 and 1.1 eV.<sup>32,33</sup> On the other hand, experimental studies on the properties of intentional doped impurities have been limited for *h*-BN.<sup>4,5,34–36</sup> Prior studies seem to indicate that p-type conductivity is easier to realize in *h*-BN than in AlN via Mg doping, revealing the potential of *h*-BN to extending p-type III-nitride materials all the way up to 6 eV.<sup>4,5,34</sup> The suitability of Si as an n-type dopant in *h*-BN has also been investigated,<sup>35,36</sup> however, yielding controversial results with its activation energy, in one case of about 1.2 eV (Ref. 35) and of about 180 meV in another.<sup>36</sup> A more recent theoretical study has indicated that substitutional carbon, carbon occupying boron site ( $C_B$ ), is a donor in monolayer *h*-BN.<sup>37</sup> The calculated activation energy ( $E_D$ ) of  $C_B$  donors in monolayer *h*-BN is about 0.94 eV.<sup>37</sup> However, the binding energy of donors (and acceptors) is expected to increase as the dimensionality of *h*-BN scales from the bulk to the monolayer due to the enhanced in-plane overlap among carriers and impurities, as well as the reduced screening. In theory,  $E_D$  will increase by a factor of 4 as the dimensionality of a semiconductor scales from the bulk to 2D, which implies that  $E_D$  could be as low as 0.24 eV in bulk *h*-BN. This argument makes carbon a possible viable candidate for n-type doping in *h*-BN. In this work, we have conducted a preliminary investigation on intentional carbon doping by metal-organic chemical vapor deposition (MOCVD) growth and determined the energy levels of substitutional carbon impurities in *h*-BN epilayers via photocurrent excitation spectroscopy.

Epitaxial layers of carbon doped *h*-BN epilayers (*h*-BN:C) employed in this study were synthesized by MOCVD using triethylboron (TEB) and ammonia ( $NH_3$ ) as the precursors for B and N, respectively. Propane ( $C_3H_8$ ) was used as the precursor for carbon doping. The basic layer structures of *h*-BN epilayers used in this study are shown in Fig. 1(a). A

<sup>a)</sup>Email: hx.jiang@ttu.edu

low temperature BN buffer layer of about 5 nm in thickness grown at 600 °C was first deposited on *c*-plane single crystal sapphire prior to the growth of the *h*-BN epilayer. The major benefits of this low temperature buffer layer include reducing the lattice mismatch between sapphire and *h*-BN, protecting the integrity of the sapphire surface at higher growth temperatures, and enhancing the adhesion of the subsequent epilayers. An undoped *h*-BN epilayer of about 30 nm in thickness was then deposited on the buffer layer at 1300 °C to serve as a template. This was then followed by the growth of a 30 nm thick *h*-BN:C epilayer at the same growth temperature. All layers were grown using hydrogen as a carrier gas. Similar to previous studies,<sup>38–40</sup> high resolution x-ray photoelectron spectroscopy (XPS) measurements were employed to estimate the carbon doping concentration ( $N_C$ ) and  $N_C$  is around  $1 \times 10^{21} \text{ cm}^{-3}$  as determined from XPS tight scans after removing surface contaminants by Ar<sup>+</sup> ion sputtering. Undoped *h*-BN epilayers with a thickness of about 60 nm were also grown at the same growth conditions for comparison measurements.

For the photocurrent excitation spectroscopy measurements, photodetectors based on a metal-semiconductor-metal (MSM) architecture with micro-strip interdigital fingers were fabricated from *h*-BN and *h*-BN:C epilayers.<sup>7,22</sup> The photolithography technique was used to pattern the interdigital fingers on the surface of *h*-BN and *h*-BN:C epilayers. Contacts consisting of bi-layers of Ti/Al (20 nm/30 nm) were deposited by e-beam evaporation for the application of bias voltages and the collection of the charge carriers (or photocurrent). The MSM detector has a device size of 0.5 mm × 0.5 mm with metal strips of 6 μm in width and spacing between the metal strips of 9 μm. A broad light source covering the wavelength range between 170 and 2100 nm [model E-99 laser-driven light source (LDLS) by Energetiq] coupled with a triple grating monochromator (Pro 2300 I of Acton by Research Corporation Spectra) was used as a variable wavelength excitation source. A source meter was used to apply voltages, and an electrometer was used to record the currents. The measurement system provides an overall spectral resolution of about 0.04 eV near the spectral region of 250 nm.

Figure 1(b) shows the room temperature photocurrent excitation spectra of *h*-BN:C and *h*-BN epilayers measured at a bias voltage of 100 V corresponding to an applied electric

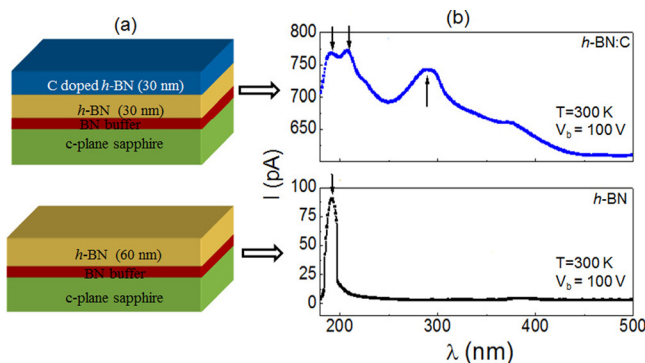


FIG. 1. (a) Schematic layer structures of samples used in this study. (b) Room temperature photocurrent excitation spectra of *h*-BN and *h*-BN:C epilayers measured at a bias voltage of  $V_b = 100$  V.

field of  $1.1 \times 10^5$  V/cm. The results clearly show that carbon doping introduces additional spectroscopic features in the spectrum of *h*-BN:C compared to that of undoped *h*-BN. The transition peaks in a photocurrent excitation spectrum is a result of carriers making transitions from different energy levels to the conduction or the valence band. For instance, one can directly excite electrons from the valence band to the conduction band. In such a context, the transition peak corresponds to the bandgap and the photocurrent is resulted from both electron conduction and hole conduction. On the other hand, in doped semiconductors, one can directly excite electrons from neutral donors ( $D^0$ ) to the conduction band, in which case the transition peak corresponds to the energy level of donors and the photocurrent is contributed by electron conduction. If a large number of ionized donors ( $D^+$ ) are present, it is also possible to excite electrons from the valence band to be captured by  $D^+$  and leave behind an equal number of holes. In this case, the transition peak is the measure of the energy difference between the donor level and the valence band, and the photocurrent is contributed by hole conduction.

Figure 2 shows a replot of the photocurrent excitation spectrum of the *h*-BN:C sample shown in Fig. 1(b) with the energy positions marked for the dominant transitions. Transition peaks observed at about 4.2, 6.0, and 6.45 eV are clearly resolved in the spectrum of the *h*-BN:C sample, while the spectrum of the undoped *h*-BN sample shown in the bottom panel of Fig. 1(b) exhibits primarily one transition peak at about 6.45 eV. The 6.45 eV transition peak can be assigned to the direct band-to-band excitation in *h*-BN epilayers and corresponds well to the previously observed optical absorption edge at around 6.4 eV (Refs. 17 and 18) and is also consistent with the room temperature energy bandgap of 6.42 eV obtained from a previous photocurrent excitation spectroscopy measurement.<sup>22</sup> The transition lines at about 4.2 eV and 6.0 eV are absent in undoped *h*-BN and are only associated with carbon doping. However, the difference between the observed bandgap energy at 6.45 eV and the transition line at 4.2 eV corresponds well to the previously measured energy

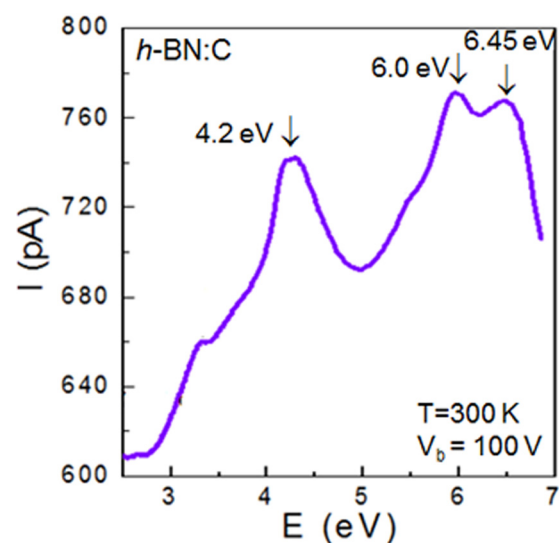


FIG. 2. Replot of the room temperature photocurrent excitation spectrum of the *h*-BN:C epilayer measured at  $V_b = 100$  V with energy peak positions marked.



with the value deduced from the temperature dependent resistivity. The present study further confirms that the room temperature bandgap of *h*-BN is somewhere in between 6.42 and 6.45 eV, and the C<sub>N</sub> deep acceptors have an energy level of about 2.2–2.3 eV. The determination of these parameters has important consequences on the basic understanding and potential applications of *h*-BN epilayers.

The MOCVD growth effort was supported by ARO (W911NF-16-1-0268) and monitored by Dr. Michael Gerhold. The detector fabrication and characterization efforts are supported by the DOE NNSA SSAA program (DE-NA0002927). Jiang and Lin are grateful to the AT&T Foundation for the support of Ed Whitacre and Linda Whitacre endowed chairs.

<sup>1</sup>Y. Kubota, K. Watanabe, O. Tsuda, and T. Taniguchi, *Science* **317**, 932 (2007).

<sup>2</sup>K. Watanabe, T. Taniguchi, T. Niiyama, K. Miya, and M. Taniguchi, *Nat. Photonics* **3**, 591 (2009).

<sup>3</sup>K. Watanabe, T. Taniguchi, and H. Kanda, *Nat. Mater.* **3**, 404 (2004).

<sup>4</sup>R. Dahal, J. Li, S. Majety, B. N. Pantha, X. K. Cao, J. Y. Lin, and H. X. Jiang, *Appl. Phys. Lett.* **98**, 211110 (2011).

<sup>5</sup>S. Majety, J. Li, X. K. Cao, R. Dahal, B. N. Pantha, J. Y. Lin, and H. X. Jiang, *Appl. Phys. Lett.* **100**, 061121 (2012).

<sup>6</sup>T. Sugino, K. Tanioka, S. Kawasaki, and J. Shirafuji, *Jpn. J. Appl. Phys., Part 2* **36**, L463 (1997).

<sup>7</sup>J. Li, S. Majety, R. Dahal, W. P. Zhao, J. Y. Lin, and H. X. Jiang, *Appl. Phys. Lett.* **101**, 171112 (2012).

<sup>8</sup>B. Huang, X. K. Cao, H. X. Jiang, J. Y. Lin, and S. H. Wei, *Phys. Rev. B* **86**, 155202 (2012).

<sup>9</sup>A. K. Geim and I. V. Grigorieva, *Nature* **499**, 419 (2013).

<sup>10</sup>N. Alem, R. Ermi, C. Kisielowski, M. D. Rossell, W. Gannett, and A. Zettl, *Phys. Rev. B* **80**, 155425 (2009).

<sup>11</sup>C. R. Dean, A. F. Young, I. Meric, C. Lee, L. Wang, S. Sorgenfrei, K. Watanabe, T. Taniguchi, P. Kim, K. L. Shepard, and J. Hone, *Nat. Nanotechnol.* **5**, 722 (2010).

<sup>12</sup>A. Maity, T. C. Doan, J. Li, J. Y. Lin, and H. X. Jiang, *Appl. Phys. Lett.* **109**, 072101 (2016).

<sup>13</sup>T. C. Doan, S. Majety, S. Grenadier, J. Li, J. Y. Lin, and H. X. Jiang, *Nucl. Instrum. Methods Phys. Res., Sec. A* **748**, 84 (2014).

<sup>14</sup>B. Arnaud, S. Lebègue, P. Rabiller, and M. Alouani, *Phys. Rev. Lett.* **96**, 026402 (2006).

<sup>15</sup>B. Arnaud, S. Lebègue, P. Rabiller, and M. Alouani, *Phys. Rev. Lett.* **100**, 189702 (2008).

<sup>16</sup>L. Wirtz, A. Marini, and A. Rubio, *Phys. Rev. Lett.* **96**, 126104 (2006).

<sup>17</sup>L. Museur, G. Brasse, A. Pierret, S. Maine, B. Attal-Tretout, F. Ducastelle, A. Loiseau, J. Barjon, K. Watanabe, T. Taniguchi, and A. Kanaev, *Phys. Status Solidi RRL* **5**, 214 (2011).

<sup>18</sup>L. Museur, E. Feldbach, and A. Kanaev, *Phys. Rev. B* **78**, 155204 (2008).

<sup>19</sup>K. Watanabe and T. Taniguchi, *Phys. Rev. B* **79**, 193104 (2009).

<sup>20</sup>M. G. Silly, P. Jaffrenou, J. Barjon, J. S. Lauret, F. Ducastelle, A. Loiseau, E. Obraztsova, B. Attal-Tretout, and E. Rosencher, *Phys. Rev. B* **75**, 085205 (2007).

<sup>21</sup>X. K. Cao, B. Clubine, J. H. Edgar, J. Y. Lin, and H. X. Jiang, *Appl. Phys. Lett.* **103**, 191106 (2013).

<sup>22</sup>T. C. Doan, J. Li, J. Y. Lin, and H. X. Jiang, *Appl. Phys. Lett.* **109**, 122101 (2016).

<sup>23</sup>M. Fanciulli and T. D. Moustakas, *Physica B* **185**, 228 (1993).

<sup>24</sup>A. Zunger and A. Katzir, *Phys. Rev.* **11**, 2378 (1975).

<sup>25</sup>C. Attacalite, M. Bockstedte, A. Marini, A. Rubio, and L. Wirtz, *Phys. Rev. B* **83**, 144115 (2011).

<sup>26</sup>B. Huang and H. Lee, *Phys. Rev. B* **86**, 245406 (2012).

<sup>27</sup>V. Wang, N. Ma, H. Mizuseki, and Y. Kawazoe, *Solid State Commun.* **152**, 816 (2012).

<sup>28</sup>W. Orellana and H. Chacham, *Phys. Rev. B* **63**, 125205 (2001).

<sup>29</sup>T. Taniguchi and K. Watanabe, *J. Cryst. Growth* **303**, 525 (2007).

<sup>30</sup>I. Jimenez, A. F. Jankowski, L. J. Terminello, D. G. J. Sutherland, J. A. Carlisle, G. L. Doll, W. M. Tong, D. K. Shuh, and F. J. Himpsel, *Phys. Rev. B* **55**, 12025 (1997).

<sup>31</sup>T. B. Ngwenya, A. M. Ukpong, and N. Chetty, *Phys. Rev. B* **84**, 245425 (2011).

<sup>32</sup>X. Z. Du, J. Li, J. Y. Lin, and H. X. Jiang, *Appl. Phys. Lett.* **106**, 021110 (2015).

<sup>33</sup>X. Z. Du, J. Li, J. Y. Lin, and H. X. Jiang, *Appl. Phys. Lett.* **108**, 052106 (2016).

<sup>34</sup>H. X. Jiang and J. Y. Lin, *Semicon. Sci. Technol.* **29**, 084003 (2014).

<sup>35</sup>S. Majety, T. C. Doan, J. Li, J. Y. Lin, and H. X. Jiang, *AIP Adv.* **3**, 122116 (2013).

<sup>36</sup>B. He, M. Qiu, M. F. Yuen, and W. J. Zhang, *Appl. Phys. Lett.* **105**, 012104 (2014).

<sup>37</sup>Y. Fujimoto and S. Saito, *Phys. Rev. B* **93**, 045402 (2016).

<sup>38</sup>M. R. Uddin, T. C. Doan, J. Li, K. S. Ziemer, J. Y. Lin, and H. X. Jiang, *AIP Adv.* **4**, 087141 (2014).

<sup>39</sup>M. R. Uddin, S. Majety, J. Li, J. Y. Lin, and H. X. Jiang, *J. Appl. Phys.* **115**, 093509 (2014).

<sup>40</sup>M. R. Uddin, J. Li, J. Y. Lin, and H. X. Jiang, *J. Appl. Phys.* **117**, 215703 (2015).

<sup>41</sup>T. T. Tran, C. Elbadawi, D. Totonjian, C. J. Lobo, G. Grosso, H. Moon, D. R. Englund, M. J. Ford, I. Aharonovich, and M. Toth, *ACS Nano* **10**, 7331 (2016).

<sup>42</sup>R. Bourrellier, S. Meuret, A. Tararan, O. Stéphane, M. Kociak, L. H. G. Tizei, and A. Zobelli, *Nano Lett.* **16**, 4317 (2016).

<sup>43</sup>K. Yuge, *Phys. Rev. B* **79**, 144109 (2009).

<sup>44</sup>S. Bahandary and B. Sanyal, *Graphene-Boron Nitride Composite: A Material with Advanced Functionalities* (InTech, 2012).